THEORETICA CHIMICA ACTA

Theoret. Chim. Acta (Berl.) 62, 373–396 (1983)

A CNDO/INDO Crystal Orbital Model for Transition Metal Polymers of the 3*d* Series—The Band Structure of Nickel(II)glyoximate

Michael C. Böhm

Institut für Organische Chemie der Universität, Im Neuenheimer Feld 270, D-6900 Heidelberg, Federal Republic of Germany

The band structure of nickel(II)glyoximate has been investigated by means of an INDO crystal orbital formalism based on the tight-binding approximation. Calculations have been performed for unit cell dimensions of 3.223 Å which corresponds to the geometry of the partially oxidized chain and of 3.547 Å for the unoxidized polymer. The convergence of the lattice sums has been studied. It is shown that resonance and classical electrostatic integrals lead to a fast convergence while the exchange contributions are only slowly reduced with increasing intercell separation. The rotational profile of the title compound shows a pronounced minimum for the staggered 90° conformation; this is in line with experimental X-ray data. The conformation of the low-dimensional system is determined by the maximization of stabilizing intercell energies. The intracell stabilization is largest for an orientation where the intercell coupling is most inefficient ($\alpha = 50°-60°$). Ligand π and lone-pair bands are predicted on top of the various Ni bands in the INDO band structure calculations. This sequence is conserved even if the creation of localized 3*d* states with trapped valences upon partial oxidation is considered. The ground state of the partially oxidized polymer corresponds to a system where charge density from the ligand framework has been removed leading to a typical organic metal or semimetal. The computational results are compared with experimental observations.

Key words: Tight-binding formalism for 3*d* polymers – Band structure approach in the CNDO/INDO approximation – Nickel(II)glyoximate polymer.

0040-5744/83/0062/0373/$04.80

1. Introduction

Nickel(II)glyoximate and various derivatives with alkyl or phenyl groups belong to a class of stacked organometallic compounds that have been studied extensively in the past decade [1, 2]. The one-dimensional (1*D*) nature of the bisdiphenyl

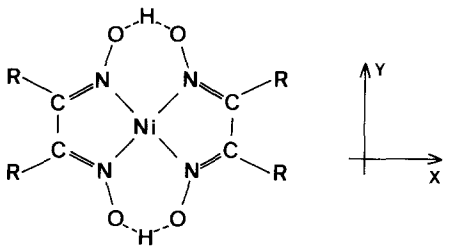

R = H, CH_3, C_6H_5

chelate complex has been recognized by Foust and Soderberg in 1967 [3]. Early contributions to the solid state and structural properties of these 1*D* Ni(II) salts have been reported in the period between 1970–1977 [4–6]. It has been shown that partial oxidation by means of I or Br leads to conductivities and transport properties that are characteristic for semiconducting materials. A detailed investigation on nickel and palladium bisdiphenylglyoximates due to the combination of various experimental techniques (e.g. X-ray, Raman spectroscopy, ESCA, UV, measurements of the conductivities, etc.) has been published in 1979 [7].

In this contribution it has been verified that the bisdiphenyl derivative of nickel(II)glyoximate forms 1*D* chains with a staggered conformation between neighbouring unit cells ($\alpha = 90°$). The NiNi distance for the neutral glyoximate system amounts to 3.547 Å [3]. This separation is reduced to 3.223 Å in the partially oxidized polymer. Acceptor moiety for the oxidation process are iodine or bromine chains that are parallel to the transition metal stacks; the halide atoms fill the tunnels in the lattice that are formed by the phenyl rings. It has been argued that the NiNi distances are too long for a direct metal coupling [7] and that charge transport processes should be traced back to the π frame of the organic ligands (for a general discussion of this subject see Ref. [8]). Raman experiments and ESCA measurements have shown that no trapped valences can be detected in the oxidized chain; thus only one oxidation state for the transition metal centers is encountered. The *dc* conductivity of the unoxidized polymer is about $8 \times 10^{-9}\,(\Omega\,\mathrm{cm})^{-1}$, copolymerization with halides leads to conductivities that span a range between $2.3\text{–}11 \times 10^{-3}\,(\Omega\,\mathrm{cm})^{-1}$ at 300 K. Detailed experimental investigations have shown that the transport properties of the 1*D* system are neither a function of the transition metal center (exchange between Ni and Pd) nor a function of the halide (I vs. Br) [7, 9]. Furthermore it has been demonstrated that I_5^- is the predominant halide component in the partially oxidized chain leading to a fractional oxidation state of +0.2 for each glyoximate moiety.

It is the purpose of this contribution to rationalize these experimental results by means of band structure calculations with the CNDO/INDO Hamiltonian

described in the preceding paper [10]. The INDO version of the semiempirical ZDO operator has been employed in the present study. The phenyl rings in the glyoximate ligands have been replaced by H atoms in the various model calculations in order to achieve matrix dimensions in the crystal orbital formalism that can be handled with available computational facilities. The remaining geometric parameters (e.g. bond lengths, bondangles, and unit cell dimensions) correspond to the experimental data of Refs. [3] and [7]. The thorough investigations in the latter publication suggest that it is not necessary to consider the halide chain in the $1D$ band structure calculations. The charge transfer in the low-dimensional system is due to the nickel(II)glyoximate stacks. Additionally there are no short distances between the Ni and the halide chains. The only function of I or Br thus is to remove electronic charge from the glyoximate donors.

In the next section the convergence of the lattice sums in nickel(II)glyoximate as derived in the INDO crystal orbital formalism is studied. We have used the experimental geometry of the partially oxidized strand with a unit cell parameter $a = 3.223$ Å and a rotational angle α of 90° between neighbouring unit cells. The rotational profile of the title compound is analyzed in Sect. 3 ($a = 3.223$ Å and $a = 3.547$ Å). The intracell and intercell energies that are determined as a function of α are divided into terms of physical significance (e.g. resonance energies, exchange contributions, and electrostatic interactions. See the preceding paper). The band structure of nickel(II)glyoximate is discussed in the following section. Detailed results for unit cell dimensions that correspond to the oxidized chain are presented for the two extreme conformations $\alpha = 0°$ (eclipsed) and $\alpha = 90°$ (staggered).

It is clear that conduction phenomena like phonon-assisted hopping or thermal activation energies that have been found in experimental studies on Ni glyoximate polymers [7] cannot be rationalized in a simple band structure description. The necessary theoretical tools for such an approach are well-known (e.g. phonon–polaron states, phonon dispersions, and solution of the Boltzmann transport equation with suitable collision term approaches) [11], the application of these sophisticated models however is prevented for unit cell dimensions encountered in the present study. Nevertheless we feel that this investigation leads to some insight into the electronic structure of the $1D$ glyoximate system, into the nature of the metal and ligand bands and into the factors that influence the geometric preferences in the polymer chain.

2. Convergence of the Lattice Sums

The sparse Extended Hückel (EH) band structure calculations that have been published for larger transition metal polymers are restricted to first or second neighbours in the lattice summations [12, 13]. Fujita and Imamura have investigated the k-dependence and the convergence of the lattice sum in polyethylene in the CNDO/2 approximation [14]. Karpfen [15] as well as Kértesz, Koller and Ažman [16] reported analytic results derived from *ab initio* tight-binding approaches. It has been shown that the k-dependence of the band structure data

Number of neighbours	E_{tot} (eV)	$\varepsilon_{val}^{bottom}$ (eV)	ε_{val}^{top} (eV)	$\varepsilon_{con}^{bottom}$ (eV)	ε_{con}^{top} (eV)	q_{Ni}	q_N	q_O	q_C	q_{Hc}	q_{Hbr}
1	−3643.9065	−10.71	−9.79	−2.64	−2.48	0.956	−0.214	−0.544	0.181	0.144	0.389
2	−3644.0208	−10.60	−9.68	−2.71	−2.55	0.954	−0.211	−0.538	0.172	0.144	0.390
3	−3644.1970	−10.71	−9.58	−2.71	−2.54	0.954	−0.212	−0.539	0.173	0.144	0.390
4	−3644.3171	−10.63	−9.49	−2.71	−2.55	0.954	−0.212	−0.539	0.173	0.144	0.390
5	−3644.4173	−10.69	−9.43	−2.71	−2.55	0.954	−0.212	−0.539	0.173	0.144	0.390
6	−3644.4748	−10.62	−9.37	−2.70	−2.55	0.954	−0.212	−0.539	0.173	0.144	0.390
7	−3644.5460	−10.67	−9.32	−2.70	−2.55	0.954	−0.212	−0.539	0.174	0.144	0.390
8	−3644.6154	−10.63	−9.28	−2.69	−2.55	0.954	−0.212	−0.538	0.174	0.144	0.390

is weak while enhanced problems are encountered with respect to the convergence of the lattice sums [14–16]. Therefore we have only studied the latter problem. In all examples, ten k-points within the first Brillouin zone have been considered. This is an upper limit as the time-consuming step in semiempirical band structure calculations on systems with larger unit cells lies in the diagonalization of the complex Hermitian matrices.

The Fourier-transformed nature of the basis equations in the tight-binding approximation is responsible for the fact that some of these sums change sign in the interval π/j (j = number of neighbours considered in the lattice sum). A necessary condition for band structure calculations is therefore a preponderance of the number of k-points in comparison to the number of neighbours.

The INDO tight-binding results for nickel(II)glyoximate are summarized in Table 1. We have displayed the total energy of the polymer, the top and the bottom of the valence and conduction bands as well as the calculated net charges [17] as a function of the number of neighbouring cells j ($j = 1$–8) considered in the lattice summations. It is seen that the net charges are only slightly modified for j dimensions beyond 1 or 2. A further increase in the number of neighbours does not lead to any significant modification in the calculated charge distribution. The same behaviour is observed for the position (top/bottom) of the conduction band. Larger variations are found for the valence band; both the position and the bandwidth depend on the number of neighbouring unit cells. In the first neighbour's approximation a bandwidth $\Delta\varepsilon$ of 0.92 eV is predicted while -10.71 eV and -9.79 eV are calculated for the bottom and the top of the valence band. $\Delta\varepsilon$ is enlarged to 1.26 eV in the fifth neighbour's approximation. This magnification must be traced back to an $\varepsilon(k)$ modification at the top of the band, since the j-dependence at the bottom is less pronounced. The band energies are only slightly modified if j ($j = 5$) is lowered or raised by 1 or 2. The total energies of Table 1 indicate that we are in a region of the model space where the lattice sums are converging.

The total energy of nickel(II)glyoximate in the various model calculations with the variable number of neighbours has been decomposed into intracell and intercell contributions (Table 2). The term A symbolizes the net intracell energy (E_{A_0} and $E_{A_0B_0}$ in the foregoing contribution). The intercell coupling has been divided into a resonance term B ($E^R_{A_0B_j}$), an exchange contribution C ($E^K_{A_0B_j}$), and the sum of electron–electron, electron–core and core–core interaction D ($D = E^J_{A_0B_j} + E^{EC}_{A_0B_j} + E^C_{A_0B_j}$). It is seen that the j-dependence of the various terms is smooth, almost identical parameters are calculated which are independent from the number of neighbours considered in the lattice sum. The modifications of the elements are negligible if j exceeds 3 or 4.

Significant differences with respect to the convergence properties however are diagnosed in the different integral types. Thus it is seen that the resonance energy (one-electron coupling) is the most important contribution in the first neighbour's cell, more than 75% of the net interaction energy are due to these terms. On the other hand B vanishes in the third neighbour's cell. The resonance energy

Table 2. Decomposition of the total energy of the nickel(II)glyoximate chain calculated as a function of the neighbouring unit cells considered in the lattice sums. A: total intracell energy; B: resonance energy; C: exchange energy; D: sum of the electron–electron, electron–core and core–core potential; E = B + C + D; B, C, D and E are intercell energy terms. All values in eV; $a = 3.223$ Å, $\alpha = 90°$

Number of neighbours		Interaction energy with the jth cell $j=1$	$j=2$	$j=3$	$j=4$	$j=5$	$j=6$	$j=7$	$j=8$	Net contributions
1	A									−3637.7607
	B	−4.7194								−4.7194
	C	−0.9295								−0.9295
	D	−0.4968								−0.4968
	E	−6.1457								−6.1457
2	A									−3637.8083
	B	−4.7087	−0.0052							−4.7139
	C	−0.9293	−0.2026							−1.1319
	D	−0.4572	0.0905							−0.3667
	E	−6.0952	−0.1173							−6.2125
3	A									−3637.7977
	B	−4.7117	−0.0052	0.00						−4.7169
	C	−0.9295	−0.2025	−0.1573						−1.2893
	D	−0.4654	0.0914	−0.0191						−0.3931
	E	−6.1066	−0.1163	−0.1764						−6.3994
4	A									−3637.8008
	B	−4.7109	−0.0052	0.00	0.00					−4.7161
	C	−0.9294	−0.2025	−0.152	−0.1250					−1.4141
	D	−0.4629	0.0911	−0.0191	0.0048					−0.3861
	E	−6.1032	−0.1161	−0.1763	−0.1202					−6.5163
5	A									−3637.7998
	B	−4.7111	−0.0052	0.00	0.00	0.00				−4.7164
	C	−0.9294	−0.2025	−0.1572	−0.1249	−0.0981				−1.5122
	D	−0.4637	0.0912	−0.0191	0.0048	−0.0021				−0.3890
	E	−6.1043	−0.1165	−0.1763	−0.1201	−0.1002				−6.6176

6	A									−3637.7794
	B	−4.7110	−0.052	0.00	0.00	0.00	0.00			−4.7162
	C	−0.9295	−0.2024	−0.1573	−0.1249	−0.0981	−0.0812			−1.5912
	D	−0.4632	0.0933	−0.0195	0.0049	−0.0022	0.0007			−0.3859
	E	−6.1037	−0.1144	−0.1768	−0.1200	−0.1003	−0.0805			−6.6933
7	A									−3637.7790
	B	−4.7111	−0.0052	0.00	0.00	0.00	0.00	0.00		−4.7163
	C	−0.9295	−0.2025	−0.1572	−0.1249	−0.0981	−0.0812	−0.0708		−1.6642
	D	−0.4634	0.0933	−0.0195	0.0049	−0.0022	0.0007	−0.0005		−0.3866
	E	−6.1039	−0.1144	−0.1767	−0.1200	−0.1003	−0.0805	−0.0713		−6.7671
8	A									−3637.7781
	B	−4.7110	−0.0052	0.00	0.00	0.00	0.00	0.00	0.00	−4.7162
	C	−0.9295	−0.2025	−0.1572	−0.1249	−0.0981	−0.0812	−0.0708	−0.0706	−1.7347
	D	−0.4632	0.0933	−0.0195	0.0049	−0.0022	0.0007	−0.0005	0.0001	−0.3859
	E	−6.1037	−0.1144	−0.1767	−0.1200	−0.1003	−0.0805	−0.0713	−0.0705	−6.8369

between the reference cell and the second nearest neighbour contributes only by an amount of about 5% to the net coupling energy. The variation of the classical electrostatic components (electron–electron, electron–core and core–core) in the lattice sum is without any problem. It is recognized that D changes sign from cell to cell in the 90° conformation of nickel(II)glyoximate (e.g. bonding with respect to the first neighbour, antibonding with respect to the second one, etc.). Significant contributions to the energy balance are found for the two nearest neighbours. The interaction energy to the fourth cell is smaller than 0.01 eV. The convergence of the exchange integrals C on the other hand is rather slow. The origin of this behaviour has been clarified in a recent semiempirical study [14]. The total exchange interaction with respect to the first neighbour amounts to -0.93 eV. This value drops below $|0.1|$ eV ($\approx$10 kJ/mol) for the coupling with the fifth cell. A large reduction is only encountered in the C terms between $j = 1$ and $j = 2$, and the other changes are small in comparison to this modification.

The INDO crystal orbital results summarized in Tables 1 and 2 suggest that the inclusion of five neighbours should be a suitable approximation in the following band structure calculations where the conformational behaviour and the $\varepsilon(k)$ shape of the glyoximate chain is studied in detail. The chosen number of k-points ($k = 10$) and neighbours in the lattice sum ($j = 5$) should be a reliable compromise between the time requirement for the matrix diagonalizations (k-restriction) and the necessary (Fourier-transforms of the integrals) balance between k and the number of neighbours (j-restriction).

3. The Conformational Behaviour of the Glyoximate Chain

The rotational profile of the nickel(II)glyoximate chain has been determined for unit cell dimensions $a = 3.223$ Å (corresponds to the NiNi separation of the partially oxidized polymer) and $a = 3.547$ Å (unoxidized glyoximate) [7]. The remaining geometric parameters of both sets of calculations are identical and have been adopted from Ref. [7]. Thus we have employed a NiN distance of 1.868 Å, a CN separation of 1.33 Å and a NO distance of 1.34 Å. The CC bondlengths in the chelate ligands are rather long (1.61 Å). We have assumed a symmetric OHO moiety with an OO distance of 2.40 Å and HO bonds of 1.22 Å. The glyoximate ligands are nonplanar; the coordinated N atoms are displaced 0.12 Å above and below the mean molecular plane. The C atoms in the chelate rings show displacements of 0.2 Å. The spatial point group of the nickel(II)glyoximate molecule is therefore D_2. The rotational profiles of the title compound for the two aforementioned unit cell dimensions are displayed in Fig. 1 (left side: $a = 3.223$ Å; right side: $a = 3.547$ Å). The relative energy for the mutual rotation of the chelate ligands has been decomposed into intracell and intercell contributions. It is seen that the staggered 90° conformation corresponds to the calculated energy minimum, a theoretical result that is in line with the experimental X-ray data [7]. The calculated energy gap between the 90° chain and the eclipsed ($\alpha = 0°$) conformation amounts to 0.775 eV in the polymer with $a = 3.223$ Å, and to 0.467 eV for the larger unit cell dimension. Eclipsed

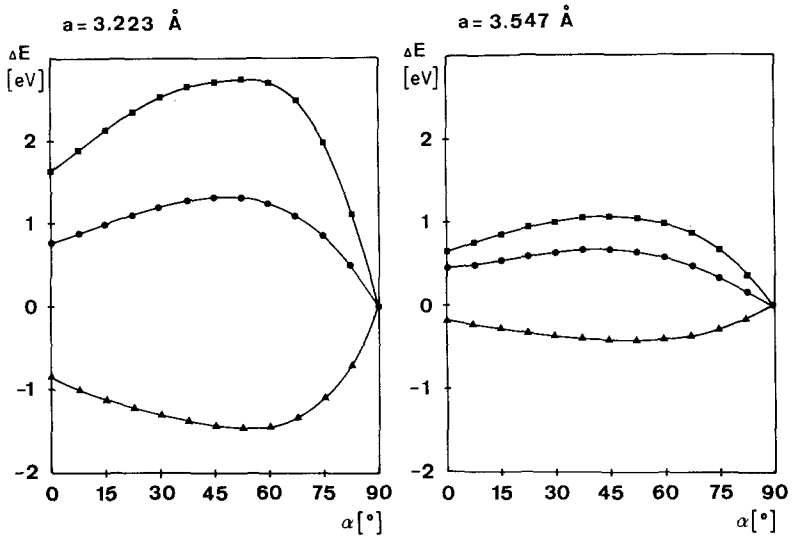

Fig. 1. Rotational barrier of nickel(II)glyoximate according to the semiempirical INDO crystal orbital model. Unit cell dimensions (a): left side = 3.223 Å; right side = 3.547 Å. The rotational barrier is given by the curves marked with the full circles; the curves with the squares correspond to the variation of the intercell potential, the triangles symbolize the variation of the intracell energy. The 90° equilibrium conformation has been used as internal standard ($\Delta E = 0$)

and staggered conformation are separated by a maximum at about 53° in the partially oxidized system and at about 38° in the unoxidized Ni polymer. The rotational barrier for the first unit cell dimension is 1.30 eV (≈ 126 kJ/mol); this gap is reduced to about one half in the latter glyoximate strand (0.66 eV ≈ 64 kJ/mol). The rotational barrier is furthermore smoothed in model calculations with planar chelate ligands; the positions of the minima and maxima however are not influenced by this operation.

The computational results in Fig. 1 indicate that intracell and intercell contributions to the net rotational profile act in different directions on the energy scale. The intracell energy has a minimum for that conformation where the interfragment coupling goes to a maximum and vice versa. The intracell energies are smallest at the staggered conformation with an angle of 90°. The mutual orientation in the chain is thus predominantly determined by the intercell coupling, which favours the staggered arrangement between neighbouring unit cells. The various curves for the $a = 3.547$ Å polymer are smooth in comparison to the energy width in the oxidized chain. The minimum and the maximum of the intercell contributions are separated by 2.75 eV, while an interval of 1.46 eV is found in the intracell potential ($a = 3.223$ Å). The corresponding values for $a = 3.547$ Å anount to 1.07 eV and 0.43 eV, respectively.

The interaction energy between the reference cell and the neighbouring moieties has been decomposed into a resonance, an exchange and a classical electrostatic (electron–electron, electron–core, core–core) component. The various contributions are displayed in Figs. 2 ($a = 3.223$ Å) and 3 ($a = 3.547$ Å) as a function of

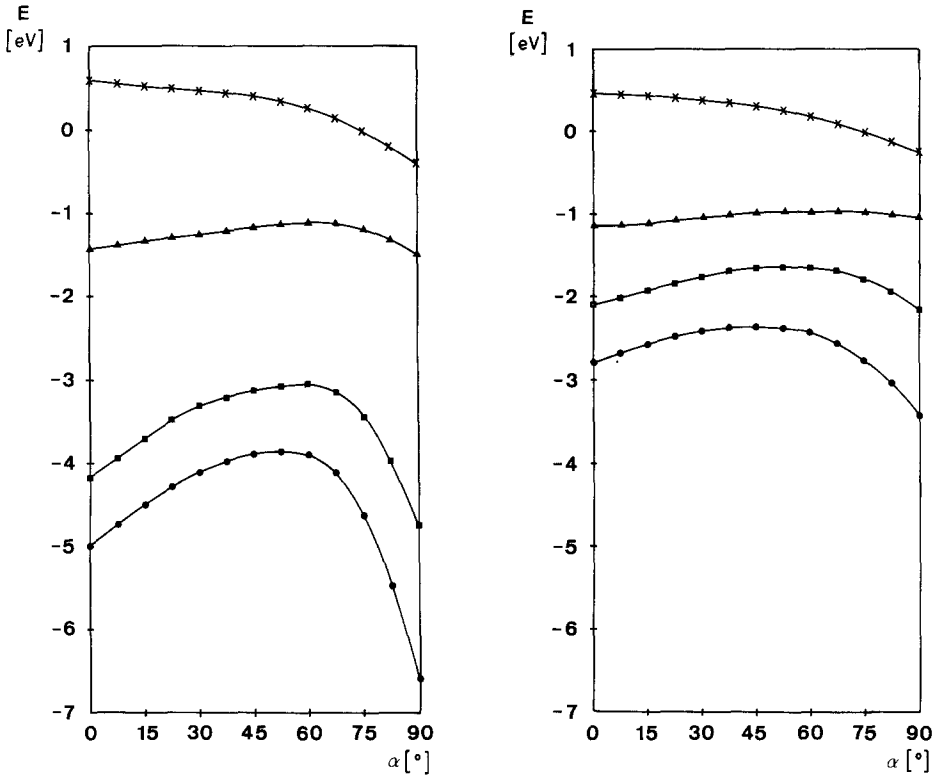

Fig. 2. Decomposition of the intercell potential for the mutual rotation of the glyoximate cells ($a = 3.223$ Å). The net intercell variation is labeled with circles. Squares: resonance contribution; triangles: exchange interaction; crosses: electrostatic energy, sum of electron–electron, electron–core and core–core coupling

Fig. 3. Decomposition of the intercell potential for a unit cell dimension $a = 3.547$ Å; see legend to Fig. 2

the rotational angle α. A detailed fragmentation scheme for the intercell elements for $a = 3.223$ Å is summarized in Table 3. The general shape of the interfragment contribution to the rotational profile is largely determined by the resonance energies; the α-dependence of the exchange and electrostatic contributions is less pronounced. The net electrostatic energy for both series of calculations is repulsive for the eclipsed 0° conformation but slightly attractive for the staggered orientation. The theoretical results collected in Table 3 show that the sum of electron–electron, electron–core and core–core interaction is destabilizing to all unit cells considered in the lattice sum in the 0° conformation. The alternation of the aforementioned attractive and repulsive coupling is realized in the 90° arrangement. The 75° conformation is characterized by nearly vanishing electrostatic interaction energies to all neighbouring unit cells, bonding and antibonding contributions largely compensate each other.

Table 3. Decomposition of the intercell energies of the nickel(II)glyoximate chain as a function of the rotational angle α. B = resonance energy; C: exchange energy; D: sum of the electron–electron, electron–core and core–core potential; E = B + C + D; all values in eV. j symbolizes the jth neighbouring cell. $a = 3.223$ Å (partially oxidized chain)

α		Interaction energy with the jth cell $j=1$	$j=2$	$j=3$	$j=4$	$j=5$	Total intercell energy
0°	B	−4.1444	−0.0047	0.00	0.00	0.00	−4.1491
	C	−0.7821	−0.2485	−0.1659	−0.1249	−0.1002	−1.4216
	D	0.5463	0.0437	0.0075	0.0018	0.0005	0.5999
	E	−4.3802	−0.2095	−0.1584	−0.1231	0.0997	−4.9708
15°	B	−3.6911	−0.0045	0.00	0.00	0.00	−3.6954
	C	−0.6958	−0.2469	−0.1631	−0.1229	−0.0986	−1.3234
	D	0.5138	0.0445	0.0011	−0.0015	−0.0011	0.5480
	E	−3.8731	−0.2069	−0.1620	−0.1244	−0.0997	−4.4708
30°	B	−3.3220	−0.0041	0.00	0.00	0.00	−3.3261
	C	−0.6268	−0.2315	−0.1572	−0.1192	−0.0964	−1.2311
	D	0.4819	−0.0042	−0.0011	−0.0024	0.00	0.4645
	E	−3.4668	−0.2399	−0.1583	−0.1216	−0.0964	−4.0924
45°	B	−3.1384	−0.0043	0.00	0.00	0.00	−3.1427
	C	−0.5821	−0.2200	−0.1519	−0.1176	−0.0967	−1.1683
	D	0.4506	−0.0481	−0.0034	−0.0026	−0.0002	0.4015
	E	−3.2699	−0.2724	−0.1553	−0.1150	−0.0969	−3.9095
60°	B	−3.0632	−0.0047	0.00	0.00	0.00	−3.0679
	C	−0.5387	−0.2107	−0.1500	−0.1193	−0.0991	−1.1177
	D	0.3117	−0.0444	0.0118	−0.0019	−0.0011	0.2761
	E	−3.2902	−0.2598	−0.1382	−0.1212	−0.1002	−3.9095
75°	B	−3.4277	−0.0051	0.00	0.00	0.00	−3.4327
	C	−0.5956	−0.2046	−0.1520	−0.1229	−0.1001	−1.1752
	D	−0.0291	0.0225	0.0022	−0.0033	0.0012	−0.0065
	E	−4.0524	−0.1872	−0.1498	−0.1262	−0.0989	−4.6144
90°	B	−4.7111	−0.0052	0.00	0.00	0.00	−4.7164
	C	−0.9294	−0.2025	−0.1572	−0.1249	−0.0981	−1.5122
	D	−0.4637	0.0912	−0.0191	0.0048	−0.0021	−0.3890
	E	−6.1042	−0.1165	−0.1763	−0.1201	−0.1002	−6.6175

The partitioning of the intracell potential of the title compound as a function of α is displayed in Fig. 4 (left side: $a = 3.223$ Å; right side: $a = 3.547$ Å). The (relative) intracell energies have been decomposed into the already mentioned two-center contributions (resonance, exchange and electrostatic interaction); additionally the sum of the one-center energies (E_{A_0} in the preceding paper) has to be considered for the total energy. As in the case of the intercell parameters, a less pronounced α-dependence is again observed for the chain with the larger unit cell dimension. The intracell minima between 38° and 53° are determined by the shape of the exchange, resonance and one-center curves. The classical electrostatic contribution is smallest in the 90° conformation. The largest energy

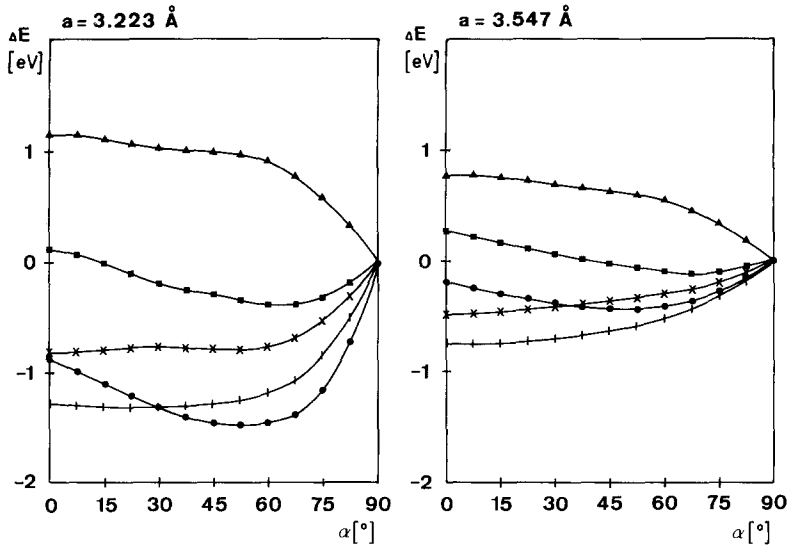

Fig. 4. Decomposition of the intracell potential for the mutual rotation of the glyoximate. Unit cell dimensions (a): left side = 3.223 Å; right side = 3.547 Å. The net intracell variation is labeled with circles. Squares: one-center energies; triangles: electrostatic energy, sum of electron–electron, electron–core and core–core interaction; crosses: resonance energy; vertical lines: exchange interaction. The 90° equilibrium geometry has been used as internal standard ($\Delta E = 0$)

variation within the intracell parameters is found for the exchange and the electrostatic interactions. The smallest α-dependence is realized for the one-center contributions while the variation of the resonance terms lies between exchange and electrostatic potential on one side and the one-center values on the other.

The α-dependence of intra- and intercell energies is of course accompanied by charge redistributions in the polymer chain. The net charges [17] for $\alpha = 0°$, 45° and 90° and $a = 3.223$ Å and $a = 3.547$ Å, respectively, are summarized in Table 4. It is seen that the electron density at the transition metal center is reduced with an increasing rotational angle. This metal-to-ligand charge shift is of greater

Table 4. Net charges of nickel(II)glyoximate for $a = 3.223$ Å and $a = 3.547$ Å as a function of α according to the INDO crystal orbital formalism

a[Å]	α[°]	Ni	N	O	C	H_C	H_{br}
3.223	0.0	0.934	−0.151	−0.423	0.048	0.142	0.402
	45.0	0.936	−0.168	−0.488	0.076	0.148	0.394
	90.0	0.954	−0.212	−0.539	0.173	0.144	0.390
3.547	0.0	0.952	−0.142	−0.483	0.042	0.143	0.401
	45.0	0.954	−0.158	−0.496	0.070	0.148	0.395
	90.0	0.963	−0.179	−0.536	0.131	0.148	0.392

br: H atom in the OHO bridge of the chelate system.

importance in the chain that corresponds to the partially oxidized polymer. Pronounced redistributions of electron density are also found in the ligand framework. The net charges at the N and O centers are enlarged in the 90° conformation while the electron population at the carbon centers is reduced. These charge shifts amount to $0.116e$ (O), $0.061e$ (N) and $-0.125e$ (C) for the glyoximate chain with $a = 3.223$ Å; the corresponding values for $a = 3.547$ Å are $0.053e$ (O), $0.037e$ (N) and $-0.089e$ (C). It is clear that the charge density at the electronegative O and N centers is depleted in the eclipsed polymer orientation due to the repulsive electrostatic intercell potential between the heteroatoms. A mutual rotation on the other hand leads to shorter distances between the electronegative heterocenters and the electropositive carbon centers.

Wiberg bond indices [18] for four glyoximate arrangements are shown in Fig. 5. The largest variations of the bond indices are found in the NO moieties, a result that is expected on the basis of the foregoing argument. The NiN indices

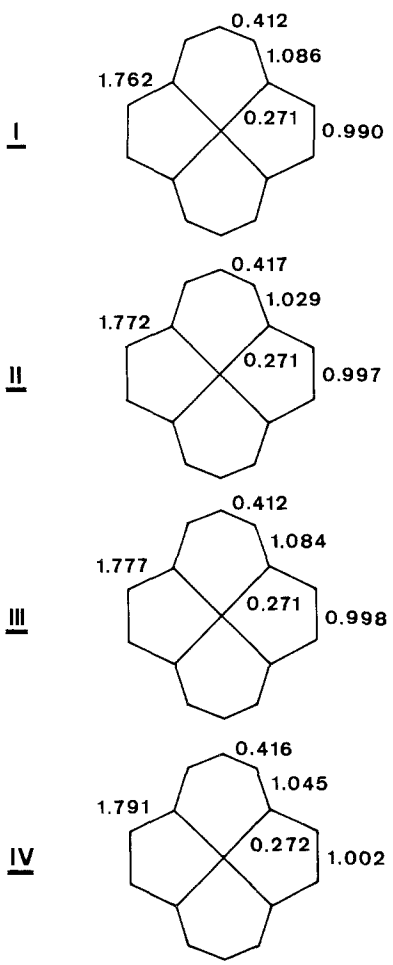

Fig. 5. Wiberg bond indices (intracell) for nickel(II)glyoximate according to the INDO crystal orbital model. I: $a = 3.223$ Å, $\alpha = 0°$; II: $a = 3.223$ Å, $\alpha = 90°$; III: $a = 3.547$ Å, $\alpha = 0°$; IV: $a = 3.547$ Å, $\alpha = 90°$

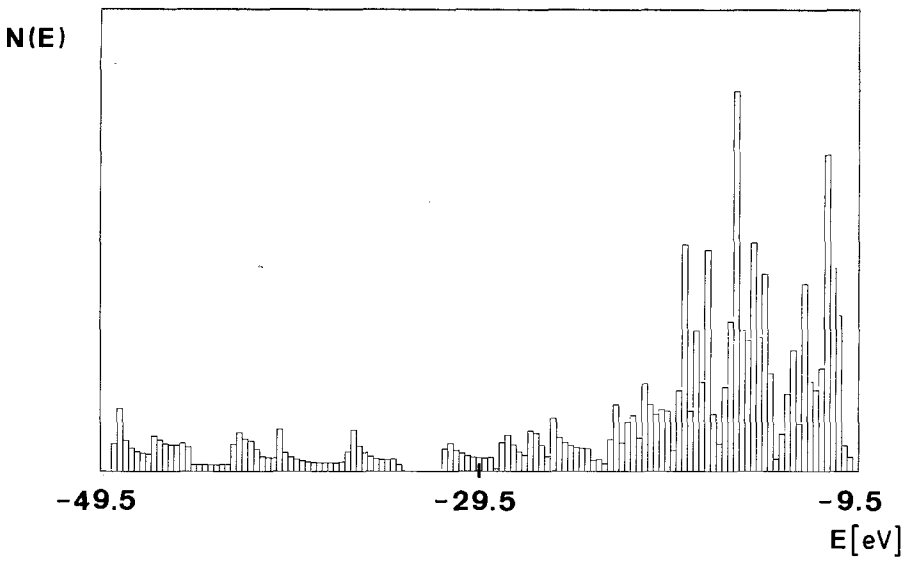

Fig. 6. Density of states for all valence bands of nickel(II)glyoximate with $a = 3.223$ Å, $\alpha = 0°$. The various bands have been approximated by fifth order polynoms, the density of states have been calculated in a mesh of 30 000 k-points for each band. The width of the energy grid amounts to 0.30 eV

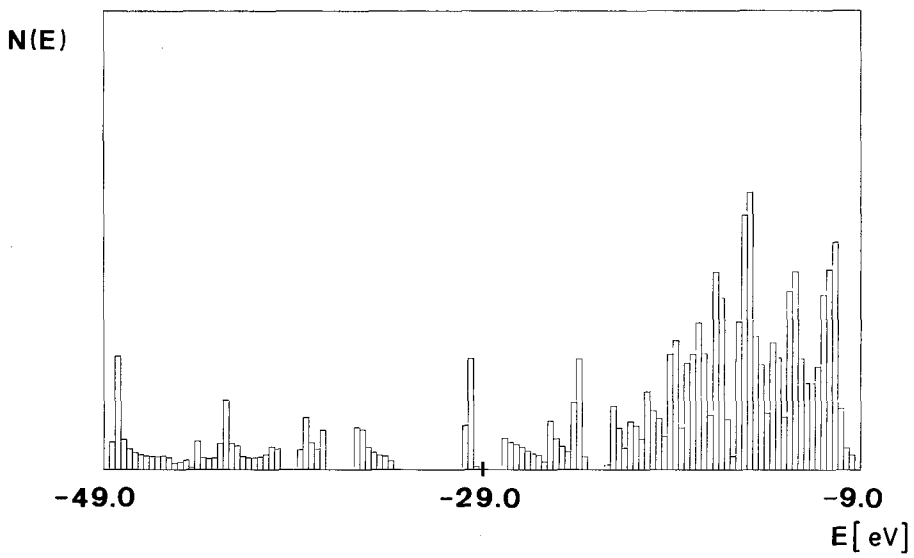

Fig. 7. Density of states for all valence bands of nickel(II)glyoximate with $a = 3.223$ Å and $\alpha = 90°$; see legend to Fig. 6

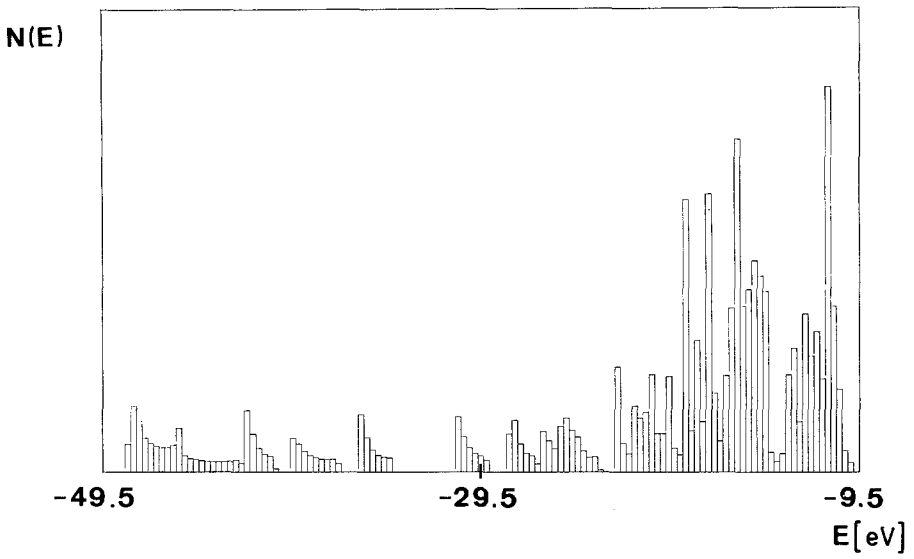

Fig. 8. Density of states for all valence bands of nickel(II)glyoximate with $a = 3.547$ Å and $\alpha = 0°$; see legend to Fig. 6

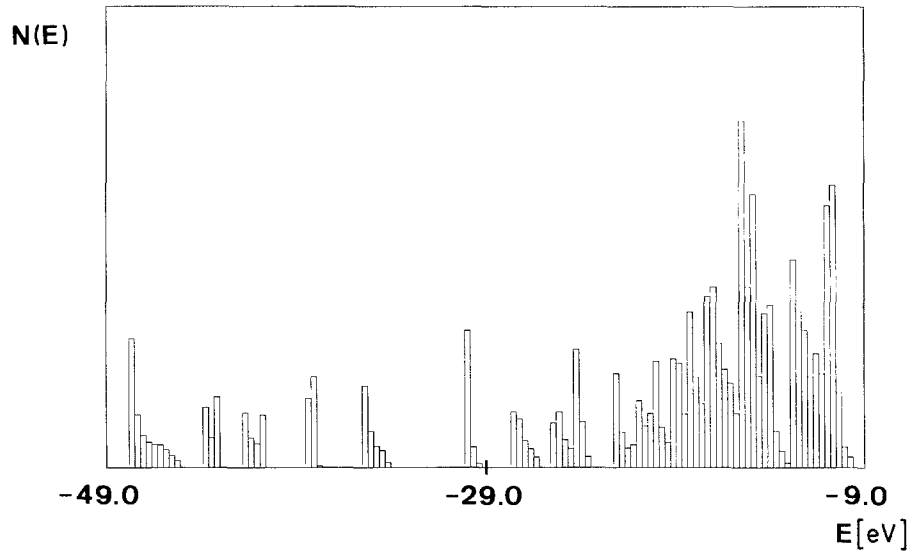

Fig. 9. Density of states for all valence bands of nickel(II)glyoximate with $a = 3.547$ Å and $\alpha = 90°$; see legend to Fig. 6

show that the transition metal ligand coupling contains significant covalent contributions. The NiNi indices between two neighbouring unit cells are small in comparison to the various intracell parameters. A bond index of 0.026 is determined for the chain with the short cell parameter, for the larger dimension a value of 0.025 is extracted from the tight-binding results ($\alpha = 90°$).

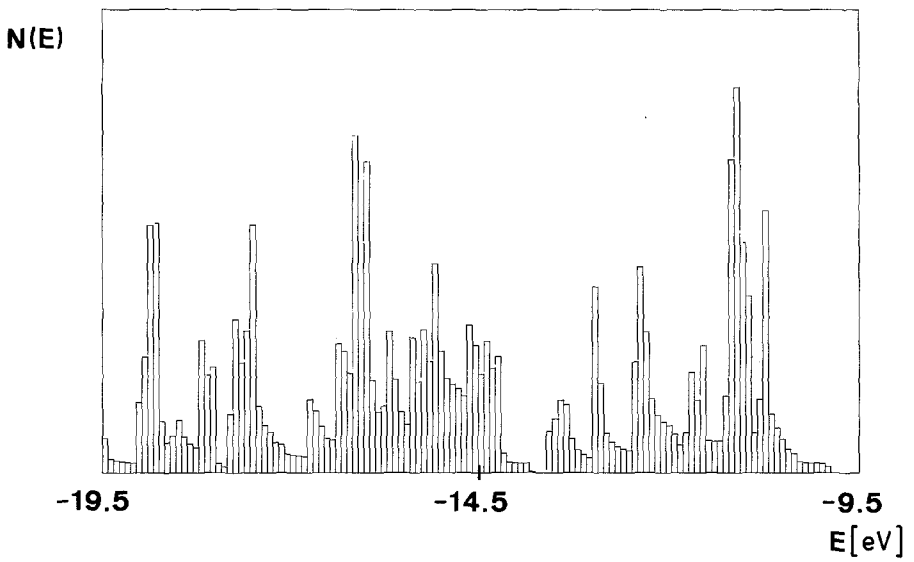

Fig. 10. Density of states of nickel(II)glyoximate with $a = 3.223$ Å and $\alpha = 0°$ in the outer valence region between -19.5 eV and -9.5 eV. The width of the energy grid is 0.10 eV

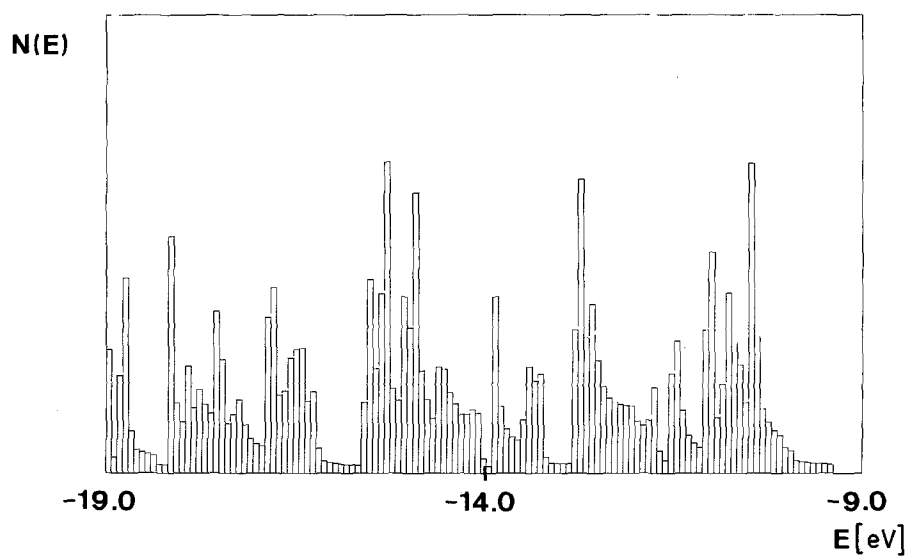

Fig. 11. Density of states of nickel(II)glyoximate with $a = 3.223$ Å and $\alpha = 90°$ in the outer valence region between -19.0 eV and -9.0 eV. The width of the energy grid is 0.10 eV

4. The Band Structure

The density of states for the occupied bands of nickel(II)glyoxime are summarized in Figs. 6–9 (Fig. 6: $a = 3.223$ Å, $\alpha = 0°$; Fig. 7: $a = 3.223$ Å, $\alpha = 90°$; Fig. 8: $a = 3.547$ Å, $\alpha = 0°$; Fig. 9: $a = 3.547$ Å, $\alpha = 90°$).

The filled bands in the 0° conformation with $a = 3.223$ Å span two regions between -34.5 eV and -48.9 eV (inner valence bands) and between -9.5 eV and -31.5 eV (middle and outer valence region). These two blocks are divided into various subunits in the staggered chain. The inner valence bands are split into three systems with approximate gaps of 1 eV and 1.4 eV, respectively. Three subunits are also found in the outer valence region, i.e. a very broad one between -9 eV and -22 eV, a smaller one between -24 eV and -28.5 eV and a narrow one above -29 eV. Larger gaps are encountered in the glyoxime polymer with the larger unit cell dimension; six blocks are found in the 0° chain (3 in the inner, 3 in the middle and outer valence region). The density of states split

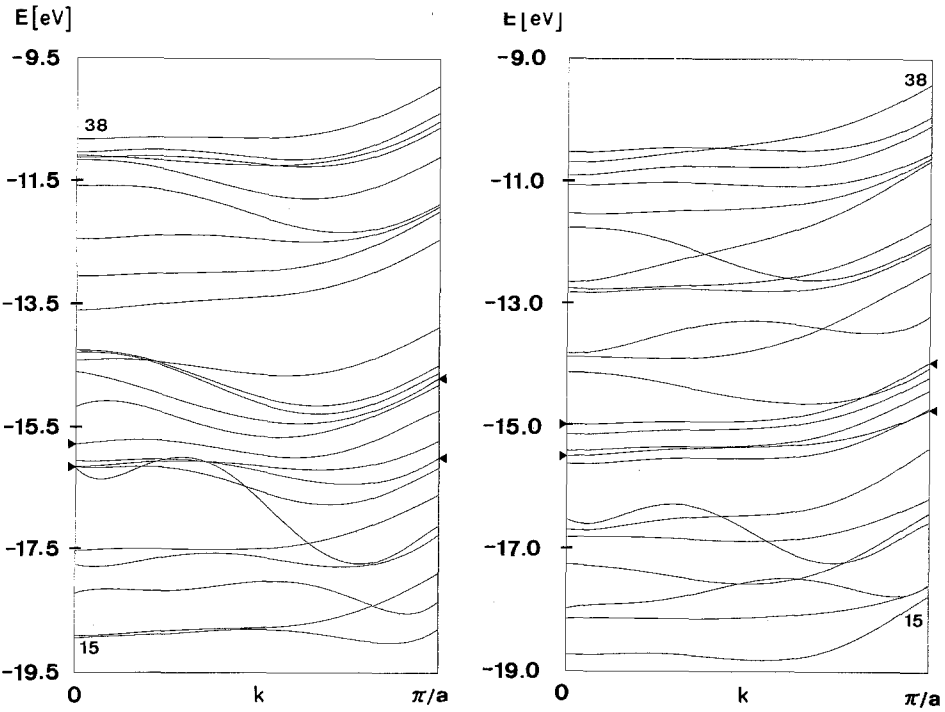

Fig. 12. The band structure of nickel(II)glyoxime with $a = 3.223$ Å and $\alpha = 0°$ in the outer valence region between -19.5 eV and -9.5 eV. The position of the bands with pronounced Ni $3d$ admixtures are labeled at the marginal k-points

Fig. 13. The band structure of nickel(II)glyoxime with $a = 3.223$ Å and $\alpha = 90°$ in the outer valence region between -19.0 eV and -9.0 eV. The position of the bands with pronounced Ni $3d$ admixtures are labeled at the marginal k-points

into 9 blocks in the 90° conformation of the glyoximate; 5 belong to the inner, and 4 to the outer region.

The density of states for the 24 highest occupied bands of the title compound in intervals between $-9/-19$ eV and $-9.5/-19.5$ eV are shown in Figs. 10–11. Only the $N(E)$ plots for the smaller ($a = 3.223$ Å) unit cell are displayed. The k-dependence of the highest occupied bands for the nickel(II)glyoximate chain with the geometric parameters $a = 3.223$ Å/$\alpha = 0°$ and $a = 3.223$ Å/$\alpha = 90°$ is presented in Figs. 12 and 13. The band structure data for these two systems are collected in Tables 5 and 6. The band energies of the conduction band at the Γ ($k = 0$) and X points ($k = \pi/a$) are also summarized in the Tables.

The density of states for both unit cell dimensions are quite similar. The correspondence between the two band structures is stronger for the eclipsed conformation, larger deviations between the oxidized and unoxidized chain are found in the staggered orientation of the chelate ligands. As a result of these similarities we can restrict the following discussion to the polymer system with the smaller unit cell dimension (3.223 Å).

The crystal symmetry of the glyoximate chain at the Γ and X points is D_2. At other k-points in the reciprocal space, the symmetry is reduced to C_2. The

Table 5. Band structure data for nickel(II)glyoximate for $a = 3.223$ Å (geometry for the partially oxidized chain) and $\alpha = 0°$ according to the INDO crystal orbital formalism. $\Delta\varepsilon$: bandwidth; ε and $\Delta\varepsilon$ in eV. The nature of the bands at $k = 0$ and $k = \pi/a$ is also displayed. L=glyoximate ligand

Band	$\varepsilon_i(0)$	$\varepsilon_i(\pi/a)$	$\Delta\varepsilon$	Character of the band at the Γ point ($k = 0$)	Character of the band at the X point ($k = \pi/a$)
39 (conduction band)	−3.18	−3.52	0.34	Ni $3d_{xy}$, $L(\pi)$, $L(\sigma)$	Ni $3d_{xy}$, $L(\pi)$, $L(\sigma)$
38 (valence band)	−10.82	−9.95	0.87	$L(\pi)$	$L(n)$
37	−11.04	−10.39	0.76	$L(\pi)$	$L(n)$
36	−11.09	−10.53	0.72	$L(\pi)$	$L(\pi)$
35	−11.13	−10.63	0.64	$L(\pi)$	$L(\pi)$
34	−11.16	−11.11	0.69	$L(n)$	$L(n)$
33	−11.58	−11.88	0.83	$L(n)$	$L(\pi)$
32	−12.45	−11.92	0.59	$L(n)$	$L(\pi)$
31	−13.06	−12.00	1.06	$L(\sigma)$, Ni $3d_{z^2}$	$L(\sigma)$, Ni $3d_{z^2}$
30	−13.61	−12.46	1.15	$L(\sigma)$	$L(\sigma)$
29	−14.26	−14.50	1.03	$L(\pi)$	Ni $3d_{yz}$
28	−14.30	−14.63	1.00	$L(\pi)$	Ni $3d_{xz}$
27	−14.43	−13.88	0.55	$L(\pi)$	$L(\sigma)$, Ni $3d_{z^2}$
26	−14.61	−14.71	0.86	$L(\pi)$	Ni $3d_{x^2-y^2}$
25	−15.16	−14.81	0.85	$L(\sigma)$	$L(\sigma)$, $L(\pi)$, Ni $3d_{z^2}$
24	−15.77	−15.23	0.77	Ni $3d_{x^2-y^2}$	$L(\sigma)$, Ni $3d_{xy}$
23	−16.06	−16.00	0.45	Ni $3d_{yz}$	$L(\pi)$, Ni $3d_{yz}$
22	−16.15	−15.72	0.43	Ni $3d_{z^2}$	$L(\pi)$, Ni $3d_{z^2}$
21	−16.16	−16.17	0.65	Ni $3d_{xz}$	$L(\sigma)$

Table 6. Band structure data for nickel(II)glyoximate for $a=3.223$ Å (geometry for the partially oxidized chain) and $\alpha=90°$ according to the INDO crystal orbital formalism. $\Delta\varepsilon$ = bandwidth; ε and $\Delta\varepsilon$ in eV. The nature of the bands at $k=0$ and $k=\pi/a$ is also displayed. L = glyoximate ligand

Band	$\varepsilon_i(0)$	$\varepsilon_i(\pi/a)$	$\Delta\varepsilon$	Character of the band at the Γ point ($k=0$)	Character of the band at the X point ($k=\pi/a$)
39 (conduction band)	−2.55	−2.71	0.16	Ni $3d_{xy}$, $L(\pi)$, $L(\sigma)$	Ni $3d_{xy}$, $L(\pi)$, $L(\sigma)$
38	−10.53	−9.95	0.58	$L(\pi)$	$L(\pi)$
37 (valence band)	−10.69	−9.43	1.27	$L(n)$	$L(\pi)$
36	−10.91	−10.10	0.82	$L(\pi)$	$L(n)$
35	−11.07	−10.55	0.54	$L(n)$	$L(n)$
34	−11.53	−10.62	0.91	$L(\pi)$	$L(n)$
33	−11.77	−12.01	0.85	$L(n)$	$L(\sigma)$
32	−12.65	−10.67	1.98	$L(\sigma)$, Ni $3d_{z^2}$	$L(\pi)$
31	−12.75	−11.68	1.07	$L(\pi)$	$L(\sigma)$, Ni $3d_{z^2}$
30	−12.82	−12.05	0.77	$L(\sigma)$	$L(\pi)$
29	−13.81	−13.20	0.61	$L(\pi)$	$L(\pi)$, Ni $3d_{xz}$
28	−13.87	−12.47	1.45	$L(\pi)$	$L(\pi)$
27	−14.12	−14.03	0.59	$L(\sigma)$, Ni $3d_{z^2}$	Ni $3d_{x^2-y^2}$, Ni $3d_{z^2}$
26	−14.96	−13.95	1.01	Ni $3d_{xz}$	Ni $3d_{yz}$
25	−15.13	−14.19	0.94	Ni $3d_{x^2-y^2}$	Ni $3d_{x^2-y^2}$, $L(\sigma)$
24	−15.39	−14.39	1.00	Ni $3d_{z^2}$	Ni $3d_{z^2}$, Ni $3d_{x^2-y^2}$, $L(\sigma)$
23	−15.47	−14.72	0.75	Ni $3d_{yz}$	Ni $3d_{xz}$
22	−15.61	−14.70	0.91	$L(\sigma)$, Ni $3d_{xy}$	$L(\sigma)$, Ni $3d_{xy}$
21	−16.53	−16.57	0.92	$L(\pi)$	$L(n)$

correlation between the irreducible representations of D_2 and C_2 is displayed below:

$$\underline{D_2} \rightarrow \underline{C_2}$$

$$A_1 \rightarrow A$$

$$B_1 \rightarrow A$$

$$B_2 \rightarrow B$$

$$B_3 \rightarrow B.$$

The contraction of the irreducible representations leads to a strong mixing of AO basis functions within the various bands. The most important consequence for the outer valence bands of the polymer lies in the allowed mixing between $3d_{xz}/3d_{yz}$ functions for k-values other than Γ and X.

The $\varepsilon(k)$ plots displayed in Figs. 12 and 13 indicate that the k-dependence for most of the bands is weak in the interval $0 \leq k \leq \pi/2a$, a stronger variation is found in the second half of the first Brillouin zone. The band structure data of Table 5 demonstrate that the highest occupied bands (calculated for a neutral

glyoximate stack, $q = 0$) are of predominant ligand character. The different composition of the various bands at $k = 0$ and $k = \pi/a$ must be traced back to the symmetry reduction for the intermediate k-points.

14 ligand bands are predicted on top of the Ni $3d$ bands in the case of the 0° conformation ($a = 3.223$ Å). This ordering scheme is comparable with the ground state MO sequence in a large number of Ni complexes (e.g. bis(π-allyl)nickel, bis(π-pentadienyl)dinickel, bis(β-dithioketonato)nickel(II)). *Ab initio* [19] and semiempirical calculations based on the present INDO parametrization [20–22] lead to ground state MO sequences where the highest ligand functions are predicted on top of the transition metal orbitals. The ligand bands of the glyoximate have been divided into π functions, oxygen lone-pair bands (n) and into ligand σ functions; the NiN orbitals belong to the latter class. The four highest occupied bands (Table 5) are of π type at $k = 0$ while the two highest ones are of predominant lone-pair character at the X point. The width of these ligand bands spans a range between 0.60–0.85 eV, the associated effective masses are between 10 and 15. The Fermi gap in the 0° conformation ($a = 3.223$ Å) amounts to 6.43 eV. The conduction band corresponds to the destabilized Ni $3d_{xy}$ combination with antibonding ligand π and ligand σ admixtures. The width of the conduction band is 0.34 eV, the effective mass is enlarged to 27.

The four occupied Ni $3d$ bands ($3d_{z^2}$, $3d_{xz}$, $3d_{yz}$, $3d_{x^2-y^2}$) for the nearly planar d^8 moiety are predicted in the region between $-15.77/-16.17$ eV (Γ point) and $-14.26/-15.27$ eV (X point). The tight-binding results show that the $3d$ bands contain negligible ligand admixtures at $k = 0$. A pronounced metal ligand coupling as well as a mixing of $3d$ AO's for nonmarginal values of the k-vector leads to switches of the relative sequence of ligand and metal bands at $k = \pi/a$. It is seen that the bandwidth of the $3d$ block and the effective masses calculated from $\Delta\varepsilon$ (e.g. $m = \hbar^2\pi^2/2a^2\Delta\varepsilon$, parabolic energy wavevector connection [23]) are far from the free electron behaviour that has been detected in the d^8 polymer of tetracyanoplatinate [24].

The tight-binding results at the 90° equilibrium geometry (Fig. 13, Table 6) differ from those derived for the eclipsed chain conformation. The mixing of ligand π and n functions is less pronounced in the staggered polymer. The width of the valence band is enlarged to 1.27 eV (effective mass: 7.1). In the energy range between -11 eV and -13 eV ligand bands are predicted where the width is increased up to 2 eV. The computational results in Table 6 indicate that the character of these broad bands differs significantly at the bottom and the top. The $\varepsilon(k)$ variation in Fig. 13 displays that this mixing is accompanied by avoided crossings of the dispersion curves.

The $3d$ block in the staggered glyoximate chain is predicted in the interval between $-14.96/-15.47$ eV at the Γ point and between $-14.03/-14.72$ eV at the X point. The k-dependence of the $3d$ bands in the first half of the Brillouin zone for the staggered chain is smaller than in the eclipsed strand. Pronounced energy shifts of the various $3d$ bands are encountered in the interval $2\pi/3a \leq k \leq \pi/a$.

The Fermi gap in the neutral nickel(II)glyoximate chain for the 90° equilibrium conformation amounts to 7.24 eV (6.43 eV in the eclipsed arrangement). The reduced bandwidth of the conduction band of 0.16 eV leads to an effective mass of 56.6 for injected particles. The calculated band gap is in line with the small conductivity (8×10^{-9} $(\Omega\,\mathrm{cm})^{-1}$) for the unoxidized bisdiphenyl derivative of the Ni chelate [7].

The band gap for both polymer conformations (eclipsed and staggered) is direct, and the highest filled level of the Ni(II) salt occurs at $k = \pi/a$; the same shape is found for the lowest vacant level in the conduction band.

The k-dependence of the calculated atomic populations for the 0° and the 90° conformation is displayed in Table 7. It is immediately realized that the AO population depends strongly on the wavevector in the eclipsed chain while the k-dependence is significantly reduced for the staggered orientation. The charge distribution at the carbon centers in the 0° chain leads to an electron deficit at $k = 0$ but to a surplus of charge at $k = \pi/a$; the opposite k-dependence in the AO population is predicted for the two heteroatoms (N, O).

Measurements of the *dc* conductivity of $Ni(dpg)_2I$ (dpg: diphenylglyoximate moiety) have shown that the partially oxidized stack has conducting properties that are typical for weak conductors or semiconductors (see discussion in the introduction). The halide chains (e.g. I) must be considered as I_5^- anions leading to a fractional oxidation state of +0.2 for each glyoximate unit. In a simple band structure picture we assume that electronic charge has been removed from the highest occupied band of the polymer (band number 37 in Table 6). The position of the Fermi level within this model is displayed in Fig. 14 where we have shown the density of states of nickel(II)glyoximate ($a = 3.223$ Å, $\alpha = 90°$) in the extreme outer valence region (hole-states and electron-states of the partially oxidized band(s) created due to the injected carriers). The Fermi energy,

Table 7. k-dependence of the calculated atomic populations of nickel(II)glyoximate for $a = 3.223$ Å and α values of 0° and 90° according to the INDO crystal orbital formalism

α	Atom	0	$20/a$	$40/a$	$60/a$	$80/a$	$100/a$	$120/a$	$140/a$	$160/a$	$180/a$
0°	Ni	9.111	9.109	9.103	9.091	9.076	9.059	9.040	9.023	9.012	9.008
	N	5.242	5.236	5.217	5.188	5.156	5.126	5.100	5.082	5.072	5.068
	O	6.512	6.511	6.505	6.495	6.482	6.467	6.450	6.436	6.425	6.421
	C	3.804	3.813	3.840	3.884	3.934	3.986	4.036	4.074	4.099	4.108
	H_C	0.861	0.861	0.860	0.860	0.859	0.858	0.857	0.856	0.855	0.855
	H_{br}	0.605	0.604	0.603	0.601	0.599	0.597	0.594	0.593	0.592	0.591
90°	Ni	9.043	9.045	9.049	9.054	9.056	9.054	9.047	9.038	9.030	9.027
	N	5.211	5.210	5.209	5.209	5.206	5.211	5.213	5.215	5.216	5.216
	O	6.535	6.534	6.534	6.536	6.538	6.540	6.542	6.545	6.546	6.547
	C	3.835	3.835	3.833	3.831	3.829	3.826	3.822	3.820	3.818	3.818
	H_C	0.856	0.856	0.856	0.856	0.856	0.856	0.856	0.856	0.856	0.857
	H_{br}	0.610	0.610	0.610	0.610	0.610	0.610	0.610	0.610	0.610	0.610

br: H atom in the OHO bridge of the chelate system.

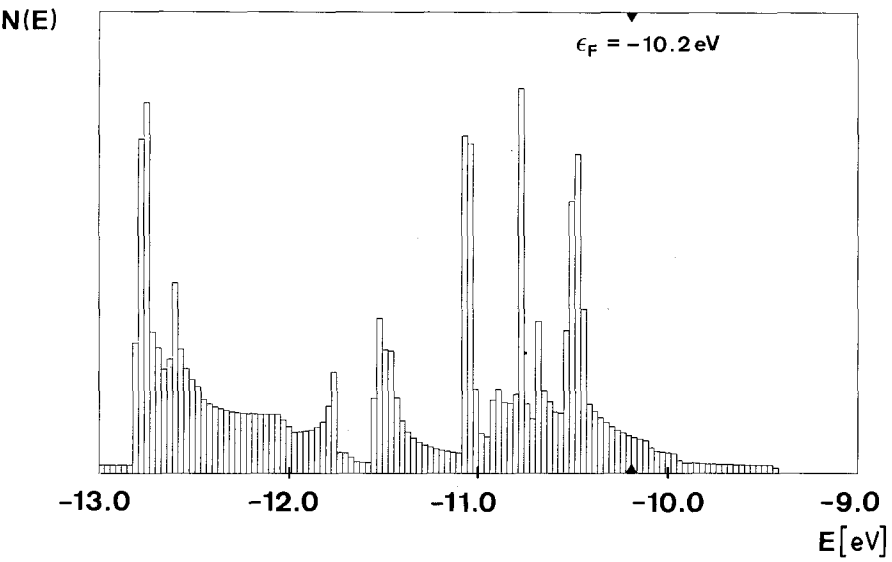

Fig. 14. Density of states of nickel(II)glyoximate in the extreme outer valence region between −13.0 eV and −9.0 eV for the staggered equilibrium conformation with $a = 3.223$ Å. The Fermi energy ε_F for the 90% filled band is displayed in the plot ($q = +0.2$ for each glyoximate moiety). The density of states have been determined in a mesh of 50 000 k-points in the first Brillouin zone. The bands have been approximated by fifth order polynoms. The width of the energy grid amounts to 0.03 eV

ε_F, for the 90% filled ligand π band amounts to −10.2 eV. This simple model is of course inadequate to rationalize the observed thermal activation energy for the charge transport. For a detailed description of these phenomena, Peierls instabilities [25], interactions of the Fröhlich type and phonon-assisted hopping has to be taken into account [26].

The theoretical prediction that the transport properties of the conducting polymer are determined by a ligand band (organic metal) is in line with the experimental observations [7]. Trapped valences in the partially oxidized chain furthermore can be ruled out on the basis of theoretical suggestions derived from the INDO tight-binding results. Two different aspects have to be considered if a charge transfer via the 3*d* bands is postulated. On one side the creation of localized states should be taken into account. Various model studies on finite transition metal compounds (binuclear and polynuclear 3*d* complexes) in the *ab initio* framework [27, 28] as well as in semiempirical LCAO approximations [29–31] have shown that cationic hole-states should be considered as localized for transition metal systems with long metal–metal bonds (>2.0Å). The symmetry adapted delocalized Hartree–Fock solution is unstable. These molecular findings of course can be extrapolated to polymer systems [32]. This means that charge transfer via the 3*d* bands in the nickel glyoximate should be always accompanied by the creation of localized electrons or holes. It is therefore only necessary to determine the reorganization energy for a localized 3*d* state in the Ni(II) salt

(second aspect). This problem is obviously intimately related to the nonvalidity of Koopman's theorem [33] in the photoelectron spectra of $3d$ complexes [34]. In a recent contribution we have shown that the reorganization energies in $3d$ complexes are comparable for topologically related compounds with similar coordination schemes of the ligands and similar oxidation states [35]. Green's function calculations on the square planar nickel(II)bis(β-dithioketonato) d^8 complex with the INDO model that is also employed in the present tight-binding calculations, lead to reorganization energies between 2.6–2.8 eV for the strongly localized Ni $3d$ levels [22]. If these increments are added to the top of the $3d$ bands encountered in the glyoximate chain ($a = 3.223$ Å, $\alpha = 90°$) hypothetic Fermi levels ε_F between -11.1 and -11.4 eV would be predicted. These estimates are in any case the upper limit for energy shifts in the partially oxidized chain. The energies are about 1 eV below the Fermi energy that has been calculated for a charge transfer from the ligand band ($\varepsilon_F = -10.2$ eV). The band sequence (ligand bands on top of Ni $3d$ bands even for oxidized chains) is therefore similar to theoretical findings in a large variety of photoelectron spectra of Ni complexes where the ground state of the cation is also formed due to a ligand hole-state [20–22, 36].

5. Conclusion

The band structure of nickel(II)glyoximate has been studied by means of semiempirical INDO calculations implemented into the crystal orbital formalism of the tight-binding approximation. It has been shown that the crystal orbital approach allowed the rationalization of various experimental results. The theoretical model should be a suitable tool for the systematic investigation of the electronic structure of recently designed low-dimensional systems with organometallic stacking units. It can be expected that such an approach facilitates the formulation of general rules and principles that determine the physical and chemical properties of quasi one-dimensional conducting or semi-conducting polymers. The large unit cell dimensions encountered in these $1D$ chains prevent the application of high quality *ab initio* models in the foreseeable future.

Acknowledgment. The work has been supported by the Stiftung Volkswagenwerk. The technical assistance of Mrs. Ingrid Grimmer in the preparation of the manuscript is gratefully acknowledged.

References

1. Keller, H. J. in: Mixed-valence compounds, Brown, D. B., Ed. Dordrecht–Boston: D. Reidel Publ. Co. 1980
2. Endres, H., Keller, H. J., Lehmann, R., Poveda, A., Rupp, H. H., Van de Sand, H.: Z. Naturforsch. **32b**, 516 (1977)
3. Foust, A., Soderberg, R.: J. Am. Chem. Soc. **89**, 5507 (1967)
4. Keller, H. J., Seibold, R.: J. Am. Chem. Soc. **93**, 1309 (1971)
5. Underhill, A. E., Watkins, D. M., Pethig, R.: Inorg. Nucl. Chem. Lett. **9**, 1269 (1973); Mehne, L. F., Wayland, B. B.: Inorg. Chem. **14**, 881 (1975); Miller, J. S., Griffiths, C. H.: J. Am. Chem. Soc. **99**, 749 (1977)

6. Gleizes, A., Marks, T. J., Ibers, J. A.: J. Am. Chem. Soc. **97**, 3545 (1977)
7. Cowie, M., Gleizes, A., Grynkewich, G. W., Kalina, D. W., McClure, M. S., Scaringe, R. P., Teitelbaum, R. C., Ruby, S. L., Ibers, J. A., Kannewurf, C. R., Marks, T. J.: J. Am. Chem. Soc. **101**, 2921 (1979)
8. Miller, J. S.: Inorg. Chem. **16**, 957 (1977)
9. Marks, T. J.: Ann. N.Y. Acad. Sci. **313**, 594 (1978); Petersen, J. L., Schramm, C. S., Stojakovic, D. R., Hoffman, B. M., Marks, T. J.: J. Am. Chem. Soc. **99**, 286 (1977)
10. Böhm, M. C.: Theor. Chim. Acta (Berl.) **62**, 351–372 (1983)
11. Suhai, S. in: Recent advances in the quantum theory of polymers. Lecture Notes in Physics, Vol. 113. Berlin: Springer Verlag 1980
12. Whangbo, M.-H., Hoffmann, R.: J. Am. Chem. Soc. **100**, 6093 (1978); Whangbo, M.-H., Foshee, M. J., Hoffmann, R.: Inorg. Chem. **19**, 1723 (1980)
13. Seelig, F. F.: Z. Naturforsch. **34a**, 986 (1979)
14. Fujita, H., Imamura, A.: J. Chem. Phys. **53**, 4555 (1971)
15. Karpfen, A.: Int. J. Quantum. Chem. **19**, 1207 (1981)
16. Kertész, M., Koller, J., Ažman, A. in: Recent advances in the quantum theory of polymers. Lecture Notes in Physics, Vol. 113. Berlin: Springer Verlag 1980
17. Mulliken, R. S.: J. Chem. Phys. **23**, 1833 (1955)
18. Wiberg, K. B.: Tetrahedron **24**, 1083 (1968)
19. Rohmer, M.-M., Veillard, A.: J.C.S. Chem. Commun. 250 (1973); Rohmer, M.-M., Demuynck, J., Veillard, A.: Theoret. Chim. Acta (Berl.) **36**, 93 (1974)
20. Böhm, M. C., Gleiter, R., Batich, C. D.: Helv. Chim. Acta **63**, 990 (1980); Böhm, M. C., Gleiter, R.: Theoret. Chim. Acta (Berl.) **57**, 315 (1980)
21. Böhm, M. C., Gleiter, R.: Chem. Phys. **64**, 183 (1982); Böhm, M. C.: Theoret. Chim. Acta (Berl.) **60**, 455 (1982)
22. Böhm, M. C.: Z. Phys. Chem. (Neue Folge) **129**, 149 (1982)
23. Ashcroft, N. W., Mermin, N. D.: Solid state physics. New York: Holt, Rinehart and Winston 1976
24. Kuse, D., Zeller, H. R.: Phys. Rev. Lett. **27**, 1060 (1971); Geserich, H. P., Hausen, H. D., Krogman, K., Stampfl, P.: Phys. Status Solidi A **9**, 187 (1972); Comès, R., Lambert, M., Launois, H., Zeller, H. R.: Phys. Rev. B **8**, 571 (1973)
25. Peierls, R. E.: Quantum theory of polymers. Oxford: Clarendon Press 1955
26. Mott, N. F.: Metal-insulator transitions. London: Taylor and Francis 1974; Shante, V. K. S.: Phys. Rev. B **16**, 2597 (1977); Bloch, A. N., Weisman, R. B., Varma, C. M.: Phys. Rev. Lett. **28**, 753 (1972)
27. Van Dam, H., Stufkens, D. J., Oskam, A., Doran, M., Hillier, I. H.: J. Electron Spectrosc. **21**, 47 (1980); Van Dam, H., Louwen, J. N., Oskam, A., Doran, M., Hillier, I. H.: J. Electron Spectrosc. **21**, 57 (1980)
28. Cox, P. A., Benard, M., Veillard, A.: Chem. Phys. Lett. **87**, 159 (1982); Benard, M.: Theoret. Chim. Acta (Berl.) **61**, 379 (1982); Newton, M. D.: Chem. Phys. Lett. **90**, 291 (1982); Messmer, R. P., Caves, T. C., Kao, C. M.: Chem. Phys. Lett. **90**, 296 (1982)
29. Böhm, M. C., Gleiter, R., Delgado-Pena, F., Cowan, D. O.: Inorg. Chem. **19**, 1081 (1980)
30. Böhm, M. C.: Theoret. Chim. Acta (Berl.) **60**, 233 (1981); Böhm, M. C.: Mol. Phys. **46**, 683 (1982); Böhm, M. C.: Int. J. Quantum Chem. submitted for publication
31. deMello, P. C., Edwards, W. D., Zerner, M. C.: J. Am. Chem. Soc. **104**, 1440 (1982)
32. Whangbo, M.-H.: J. Chem. Phys. **70**, 4963 (1979); Whangbo, M.-H.: J. Chem. Phys. **73**, 3854 (1980); Whangbo, M.-H.: J. Chem. Phys. **75**, 4983 (1981)
33. Koopmans, T.: Physica **1**, 104 (1934)
34. Cauletti, C., Furlani, I.: Struct. Bonding **35**, 119 (1980); Green, J. C.: Struct. Bonding **43**, 37 (1981)
35. Böhm, M. C.: J. Chem. Phys. in press
36. Böhm, M. C.: Z. Naturforsch. **36a**, 1361 (1981)

Received July 19/September 22, 1982